BOLLETTINO DI GEOFISICA TEORICA ED APPLICATA VOL. 45, N. 3, PP. 215-232; SEPTEMBER 2004

How good are shear wave velocity models obtained from inversion of ambient vibrations in the Lower Rhine Embayment (N.W. Germany)?

M. OHRNBERGER[1], F. SCHERBAUM[1], F. KRÜGER[1], R. PELZING[2] and S.-K. REAMER[3]

[1] *Institut für Geowissenschaften, Universität Potsdam, Germany*
[2] *Geologischer Dienst NRW, Krefeld, Germany*
[3] *Abt. für Erdbebengeologie der Universität zu Köln, Bergisch-Gladbach, Germany*

(Received June 6, 2003; accepted February 11, 2004)

Abstract - We present the results of independent tests on the reliability of shear-wave velocity models derived from ambient vibration measurements in the Lower Rhine Embayment (LRE) in north-western Germany. For one site, we compare the shear-wave velocity model obtained from active downhole measurements directly to our result of the inversion of ambient vibration data. We find a remarkably good agreement between the independently derived shear-wave velocity profiles for this site. At another location, we tested the proposed shear-wave velocity model derived from ambient vibration measurements by using local earthquake data recorded at a 350 m-deep borehole station and at a strong motion station at the surface. We tested the accuracy of the shear-wave velocity profile by modifying the shallow part of a minimum 1D reference model in the LRE, to theoretical model seismograms for a local earthquake (M_L = 4.1) and compared those to the earthquake records observed. We further computed the top/bottom spectral ratios for 11 local earthquakes and compared them to the SH transfer function predicted from the ambient vibration model. These tests show some deviation of the proposed shear-wave velocity model and the evidence obtained from the local earthquake records. The mismatch in fundamental peak frequency from 0.62 Hz predicted for the ambient vibration model to approximately 0.50-0.55 Hz obtained from the spectral ratios can be explained by an underestimation of the sediment thickness. Two strong spectral peaks were observed at 3.8 Hz and 10.2 Hz, which the model fails to predict. The limitations of the model derived from ambient vibrations can be attributed to the simplified model parametrization (smooth

Corresponding author: M. Ohrnberger, Institut für Geowissenschaften, Universität Potsdam, Karl-Liebknecht-Str. 24, D-14476 Golm b. Potsdam, Germany. Phone: +49 3319775410, Fax: +49 3319775060;
e-mail: mao@geo.uni-potsdam.de

power-law function) used in the inversion procedure. A more flexible parametrization of the model in the inversion procedure may allow for a better resolution of the very shallow and deeper parts of the velocity profiles.

1. Introduction

The effects of local subsurface structure on seismic motion, commonly expressed by the term "site effects", are well known among seismologists (e.g. Borcherdt, 1970; Campbell, 1976; ESG, 1998). Site classification and site effect estimation are major issues in seismic hazard assessment and engineering seismology. The shallow, shear-wave velocity in the upper 30 m of the sediment column, known as $v_S(30)$, in the International Building Code adopted in 2001 (BSSC, 2001) has been found to correlate with site amplification and damage distributions (e.g. Borcherdt and Gibbs, 1976; Hartzell et al., 1996). To model the strong ground motion of future, potentially hazardous earthquakes -a main target in probabilistic seismic hazard assessment studies- requires a detailed knowledge of the 3D shear wave velocity structure at greater depths as well, to allow reliable estimates of frequency-dependent site amplifications (e.g. Gao et al., 1996; Yamanaka, 1998).

The passive recording of microtremors at a single station (e.g. Bard, 1998; Ishida et al., 1998; Fäh et al., 2001) or at small-scale arrays (e.g. Horike, 1985; Tokimatsu et al., 1992; Tokimatsu, 1997; Satoh et al., 2001a, 2001b) is regarded as a low-cost option for the determination of shallow, shear-wave velocity profiles. Ambient noise measurements are easy to perform and feasible even in urban areas. However, the accuracy of the shear-wave velocity models derived from these methods is still being debated (e.g. Wills, 1998; Boore and Brown, 1998) and is the subject of on-going projects at national (Array Geophysical Research Investigations at Points of Particular Interest using Noise Analysis - AGRIPPINA, Universities of Cologne, Potsdam, Stuttgart and Munich) and international level (EU-Grant No. EVG1-CT-2000-00026: Site EffectS assessment using AMbient Excitation - SESAME).

For the Lower Rhine Embayment (LRE) in N.W. Germany, several ambient noise studies (Ibs von Seht and Wohlenberg, 1999; Parolai et al., 2002; Hinzen et al., 2003) have been performed providing shear-wave velocity depth models for the region using single station H/V ratios. In a recent paper, Scherbaum et al. (2003) showed how to obtain shear-wave velocity profiles from a combined inversion of dispersion curves and H/V ratios derived from ambient vibration recordings. As a sequel to this work, we want to answer the question: how good are those shear-wave velocity profiles when tested by independent investigations? To independently check these shear-wave velocity profiles we conducted the following tests. First, we performed additional microtremor array measurements in the LRE (see Fig. 1) at one site where the shear-wave velocity profile is independently constrained from active downhole measurements in a shallow borehole (Budny, 1984). Secondly, we installed a mid-period seismometer (type: Lennartz LE3D-5s) at the Pulheim site (PLH, see Fig. 1) between summer 2000 and summer 2001, where the Geological Survey of North-Rhine-Westfalia (GD-NRW) operates both a 3-component borehole velocity sensor at 350 m depth (station PLH) and a surface accelerometer

(station PLH-S) as part of their LRE seismic network (Pelzing, 1990). Between the year 2000 and 2002, eleven local earthquakes with a sufficiently good signal to noise ratio were recorded at these stations. One of the recorded events (M_L = 4.1) and two of its aftershocks, located between the cities of Heerlen and Kerkrade, just a few kilometers away from Aachen (Fig. 1), were also recorded on the LE3D-5s instrument. We were able to derive a full moment tensor solution for this event by inverting local and regional seismogram recordings which enabled the computation of synthetic seismograms for both the PLH and PLH-S stations. Using a regional velocity model for the crustal structure (Reamer and Hinzen, 2001) and introducing the shallow, shear-wave velocity model determined from ambient vibration data inversion for this site (Scherbaum et al., 2003), we compared the waveforms of observed and synthetic seismograms qualitatively and quantitatively. Finally, we used the records of the eleven local earthquakes to determine the spectral ratios between the surface and the borehole stations and compared them to the SH-transfer function computed for the shear-wave velocity model obtained in Scherbaum et al. (2003).

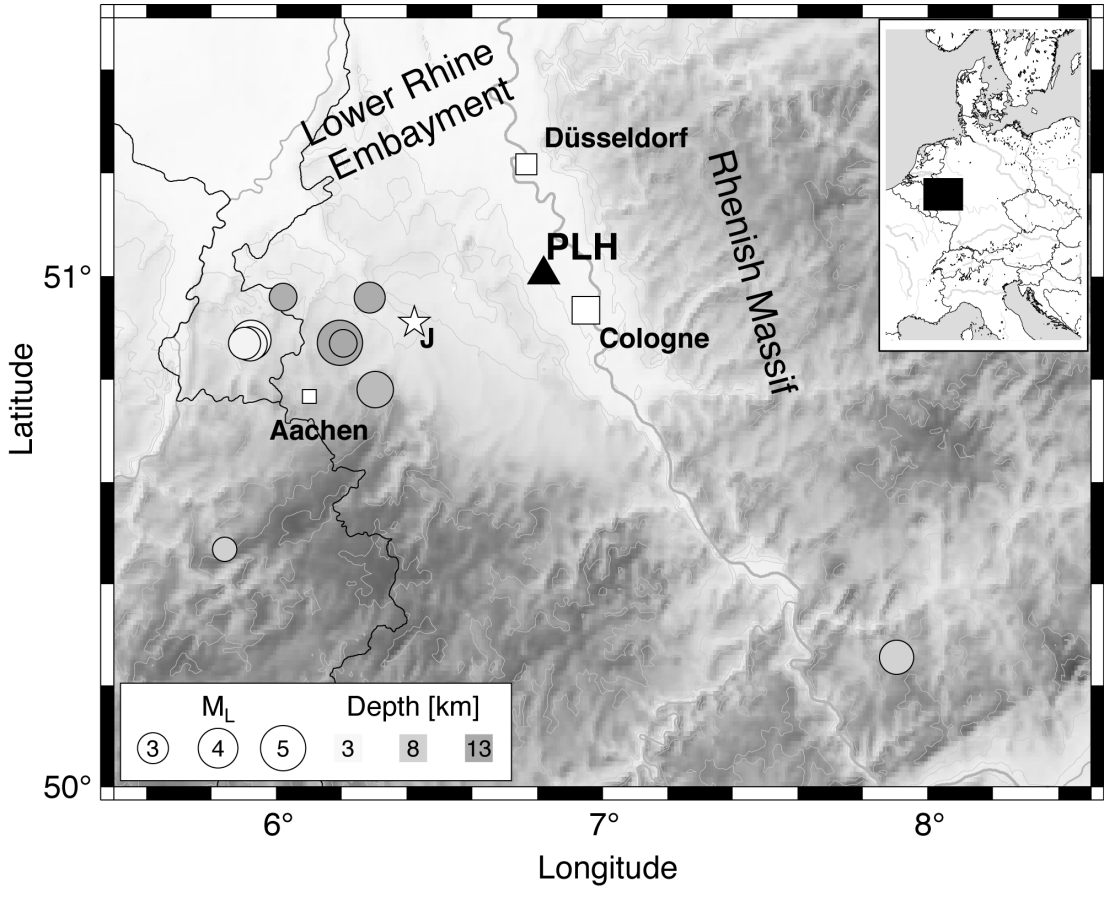

Fig. 1 - Overview of the study area in the LRE comprising the cities of Cologne, Düsseldorf and Aachen. The white star indicates the location of the Jülich (J) site, where ambient vibration measurements were performed. The location of 11 local earthquakes recorded between the year 2000 and 2002 at the PLH station (black triangle) are given by shaded circles. The symbol size is related to the local magnitude M_L and shading indicates hypocenter depth as given in the legend below.

2. Ambient noise vs. downhole measurements

In summer 2001, we performed ambient vibration array measurements at one site in the LRE. We selected the location of the Jülich (Fig. 1) measurement site on the basis of an earlier study by Budny (1984) who performed active downhole measurements for both compressional and shear-wave velocities at 36 borehole locations in the LRE. The borehole location at the Jülich site is one of the deepest boreholes where Budny (1984) reported a shear-wave velocity profile, thus enabling a direct comparison of his independently constrained results with the shear-wave velocity model derived via the combined inversion procedure proposed in Scherbaum et al. (2003).

In order to fully utilize the valid frequency range for the dispersion analysis, we used mid-period seismometers with a corner period of 5 s (type: LE3D-5s). The realized array geometry with 11 seismic stations is shown in Fig. 2. Examples of one broadband (0.2 Hz to 5 Hz) and one narrowband (1.8 Hz to 2.2 Hz) array response function (Figs. 2b and 2c) indicate the resolution capabilities of this configuration. We recorded approximately 2 hours of data at 125 Hz sampling frequency with a 120 dB resolution (Lennartz Marslite data logger). Through careful visual inspection of the data, we rejected recordings containing stronger transient bursts on any of the records. In this way, we selected seven minutes of waveform data as appropriate for the array analysis. We analyzed the vertical component data in narrow, half-overlapping and logarithmically-spaced frequency bands by a conventional f-k (frequency-wavenumber) approach (Kværna and Ringdahl, 1986) and by high-resolution f-k maximum-likelihood spectrum analysis (Capon, 1969). The frequency bandwidth as well as the time lengths of the individual analysis windows were adjusted with respect to the center period of each frequency band, resulting in a constant time-bandwidth product processing scheme for all analysis windows. Furthermore, using the same data windows as those used for the dispersion analysis, we computed H/V spectral ratios (HVSR) for all individual array stations using Welch's power spectral estimation technique (Welch, 1967) after applying a smoothing window (Konno and Ohmachi, 1998). The H-spectrum was calculated as $H = \sqrt{NE}$, that is, the geometric mean of the

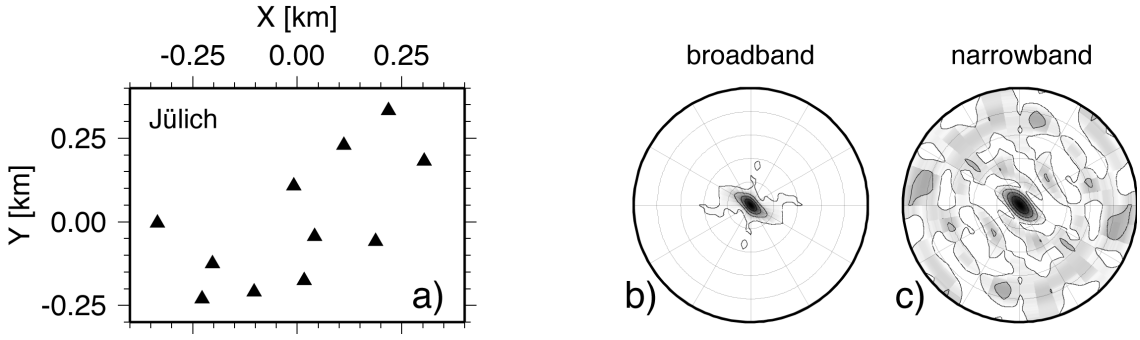

Fig. 2 - Geometry of the array configuration used in the ambient vibration measurements at the Jülich site (a) and corresponding array response functions for two frequency bands. "Broadband array response" from 0.2 Hz to 5 Hz is shown in (b), whereas (c) gives the "narrowband array response" for a center frequency of 2 Hz and a half-bandwidth of 10% (1.8 Hz-2.2 Hz).

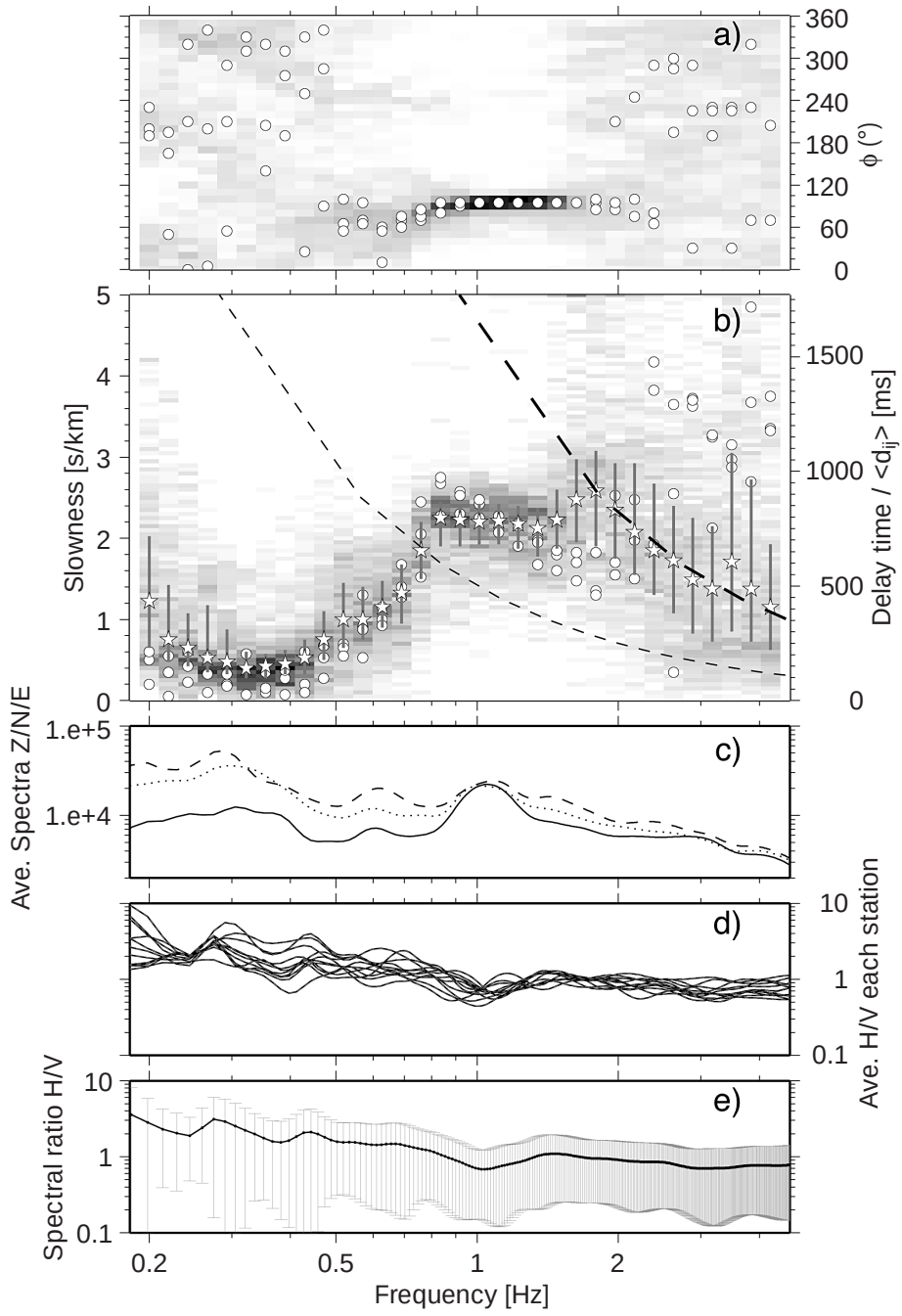

Fig. 3 - Dispersion curve analysis results from ambient vibration array measurements at the Jülich site in the LRE. Backazimuth (a) and slowness (b) estimates of individual analysis windows obtained from the conventional f-k technique summarized as histogram density plots. White stars and grey lines in (b) give the median and median deviation computed from the slowness distribution for each frequency band. White circles in (a) and (b) show estimates obtained by the high-resolution f-k method after Capon (1969). Dashed lines correspond to the aliasing condition for the minimal and average interstation distances of the realized array geometry. (c), (d), and (e) show the average spectral amplitudes observed at the array stations for individual components (solid: vertical, dashed: north, dotted: east), the individual HVSR estimates at array stations, and the average HVSR of all array stations, respectively. For details, please see text.

north and east horizontal component spectra. We then performed a combined inversion of dispersion curve results and HVSR estimates in order to obtain the best fitting shear-wave velocity model [for details, see Scherbaum et al. (2003)].

The result of the ambient vibration analysis and the combined inversion for the Jülich site are shown in Figs. 3 and 4, respectively. In the upper panels of Fig. 3, we show density plots summarizing all directional (Fig. 3a) and slowness (Fig. 3b) estimates obtained for the individual analysis windows by applying the conventional f-k algorithm. These histogram displays allowed us to check whether preferred directions in the ambient noise wavefield exist - a favorable situation for the use of the conventional f-k technique - as well as to compute first and second order statistical parameters from the slowness distributions for each frequency band. We used the median and corresponding median deviation drawn from the distributions as dispersion-curve estimates for the inversion. A visual control for the valid frequency band of dispersion-curve determination was obtained directly from the scatter of the slowness distributions. As additional control criteria, we show the limitations of the array geometry with respect to the spatial sampling of the wavefield in Fig. 3b by the aliasing curves calculated for the minimal (upper-dashed line) and average (lower-dashed line) inter-station distance between the array stations. The direction and slowness estimates from Capon's (1969) high-resolution f-k algorithm show a good agreement with the results obtained from the statistics of the conventional technique. Fig. 3c presents the average amplitude spectra from all array stations so as to provide a visual quality control of the spectral energy content of the single seismometer components, allowing one to recognize the filter effects caused by the shallow sediment structure which could limit the valid frequency band for both dispersion curve and HVSR interpretations (Scherbaum et al., 2003). HVSR for all individual array stations are given in Fig. 3d to demonstrate the absence of a large scatter within the area of the array deployment indicating the existence of a predominant one-dimensional sediment structure without large lateral heterogeneities. The input HVSR data for the combined inversion is the mean HVSR of all array stations together with the standard deviation obtained from the averaging process as error estimate (Fig. 3e).

The inversion of the dispersion curve and the HVSR data was performed using the procedure described in Scherbaum et al. (2003). That is, the velocity model class for the

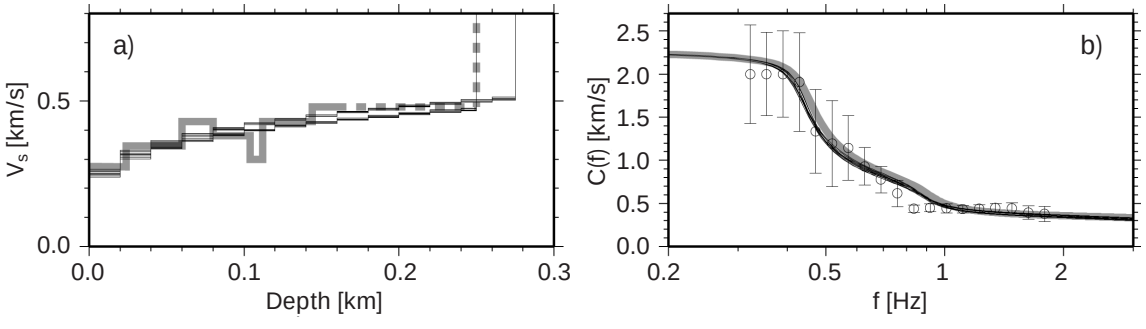

Fig. 4 - Results of combined inversion procedure following Scherbaum et al. (2003) for the Jülich site: a) comparison of the ten best-fitting shear-wave velocity models (black lines) and the V_S velocity profile derived by Budny (1984) from downhole measurements (gray line); b) fit of corresponding dispersion curves for models shown in (a).

inversion was parametrized as a single sediment layer over a halfspace, where the sediment shear-wave velocity increases with depth following a power-law function $V_S(Z) = V_{S0} Z^{\alpha}$, for depths $Z > 0$ (Z positive downward). The halfspace velocities are fixed at 2.5 km/s in all cases, and values for the compressional-wave velocities and layer densities were set according to relations given by Budny (1984) for this region. The free parameters of the inversion are the shear-wave velocity at the surface V_{S0}, the power law exponent α and the sediment thickness H. We set the frequency band used for the inversion to the range from 0.3 Hz to 1.8 Hz.

In Fig. 4a we compare the ten best-fitting shear-wave velocity profiles (black lines) obtained from the combined inversion for the Jülich site to the model derived from active downhole measurements by Budny (1984; gray line). By taking the average of the best fitting models, we obtained the following parameters for the shallow shear-wave velocity profile: surface shear-wave velocity $V_{S0} = (157 \pm 9)$ m/s, power-law exponent $\alpha = 0.206 \pm 0.012$ and the thickness of the sediment layer is estimated as $H = (264 \pm 13)$ m. The models in Fig. 4a can be compared to the maximum borehole depth of 160 m. We extended the model derived by Budny (1984) to match the sediment thickness of the inverted model in Fig. 4a for a better comparison of the corresponding dispersion curve fits shown in Fig. 4b. Considering that the parametrization scheme used for the sediment layer does not allow to invert for the small-scale velocity variations, visible in the shear-wave velocity profile of Budny (1984), we consider the correspondence between the models derived from active and passive measurements as excellent. The relative deviation between the velocity models averaged over all layers is in the order of 10% (absolute deviation: 38 m/s), whereas the average velocity in the sediment column fits to 2.5% (absolute: 10 m/s).

Table 1 - Hypocentral parameters of the local earthquake records used in this study. Distance and backazimuths are given with respect to the Pulheim site (PLH).

EVID	Origin Time	Lat [°]	Lon [°]	H [km]	M_L	Baz [°]	D [km]	REGION
0790	2000-07-26 12:19:24.4	50.256	7.905	7.8	3.4	136.9	113.5	Attenhausen
0882	2001-06-23 01:40:03.5	50.877	5.922	3.2	4.1	257.7	64.8	Kerkrade (Mainshock)
0883	2001-06-23 01:53:45.2	50.869	5.919	3.6	3.4	257.0	65.2	Kerkrade (Aftershock)
0884	2001-06-23 02:02:31.3	50.871	5.902	3.5	3.1	257.4	66.3	Kerkrade (Aftershock)
0942	2001-10-03 11:00:13.5	50.959	6.286	12.8	3.0	262.6	40.0	Linnich
0963	2001-11-10 00:44:03.6	50.961	6.020	12.4	2.6	265.4	57.8	W. Geilenkirchen
0983	2002-01-04 03:36:11.3	50.468	5.841	8.1	2.4	229.6	91.7	Spa (Belgium)
1019	2002-03-17 14:46:30.6	50.780	6.302	10.7	3.6	235.8	45.5	E.Stolberg (Hamich)
1065	2002-07-22 05:45:05.1	50.872	6.195	13.1	4.9	251.7	48.0	Alsdorf (Mainshock)
1073	2002-07-22 09:09:58.2	50.871	6.204	13.1	2.6	251.3	47.7	Alsdorf (Aftershock)
1074	2002-07-22 12:39:13.4	50.867	6.214	11.4	2.5	250.9	46.7	Alsdorf (Aftershock)

3. Local earthquake analysis: seismogram forward modeling

At Pulheim (PLH, Fig. 1), located around 20 km north-west of Cologne's city center, the GD-NRW operates a 3-component borehole velocity sensor (station PLH, $T_o = 1$ *s*, critical damping $h = 62\%$) at a 350 m depth in parallel to a surface accelerometer atop PLH (station code PLH-S). At this site, we had conducted an ambient vibration array experiment in the late summer of 2000 and derived the shallow-shear velocity structure via combined inversion of the dispersion curve and the HVSR data (Scherbaum et al., 2003). After this experiment, we continued to operate one of the array stations (station code P06G) until July 2001. Eleven local earthquakes, as listed in Table 1 and shown in Fig. 1, were recorded in the time period between July 2000 and July 2002 at stations PLH and PLH-S. One larger earthquake (*ML* = 4.1), located close to the Netherlands-German border, between the cities of Heerlen and Kerkrade, and two of its aftershocks were also recorded by our instrument (P06G).

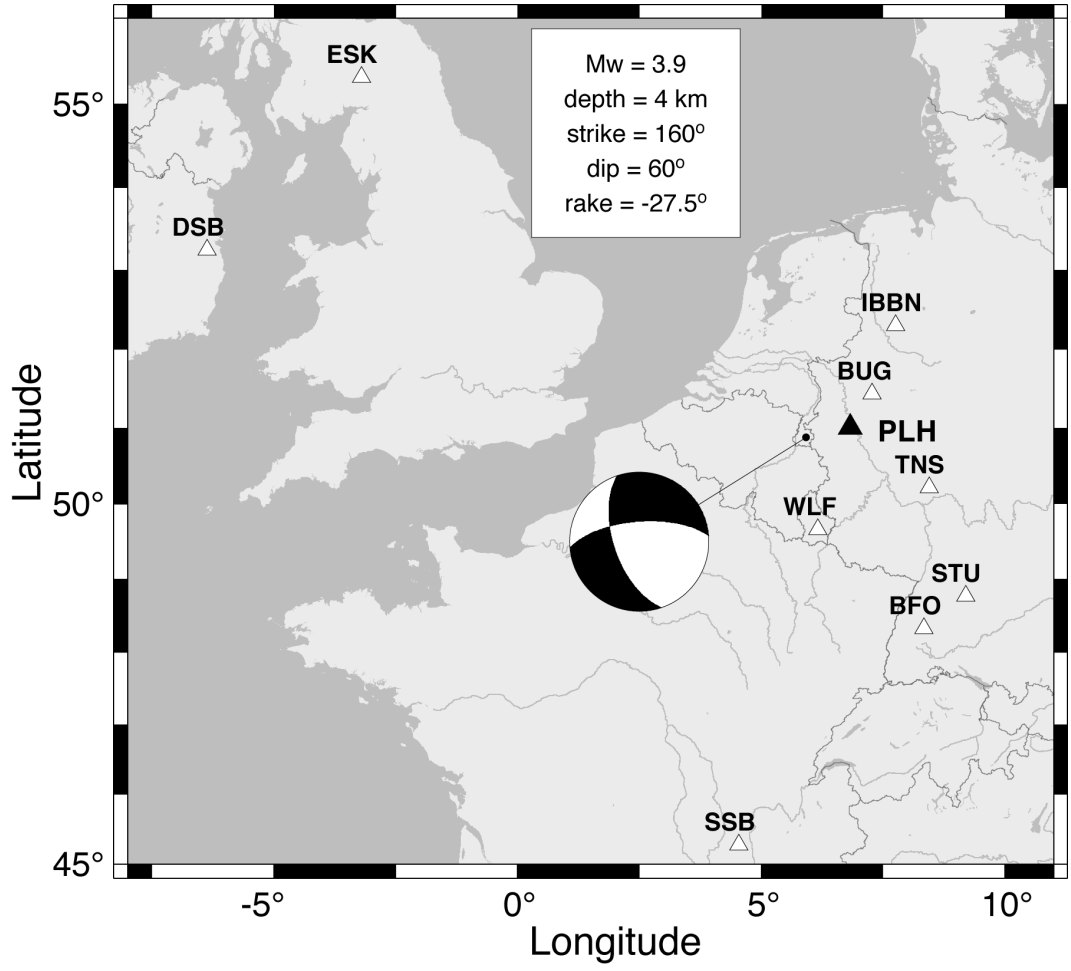

Fig. 5 - Map of station distribution used for the moment tensor inversion of the Heerlen mainshock. Inset gives the focal parameters found from inversion for this shallow normal fault event [strike, dip, rake definitions follow Aki and Richards (1980)].

We used local and regional seismogram recordings of the broadband stations shown in Fig. 5 (white triangles) to determine a full moment tensor solution for the Heerlen/Kerkrade mainshock. The inversion was carried out in the frequency domain in the period range from 20 s to 40 s by iteratively fitting the amplitude spectra of the entire seismograms and assuming a point source model. Green's functions for the inversion have been calculated using a crustal velocity model derived for Germany (Schlittenhardt, 1999). Technical details of the inversion procedure employed are given in Krüger and Dahm (2002). The parameters of the best-fitting moment tensor solution are given in the inset of Fig. 5 together with a depiction of the corresponding focal mechanism (lower hemisphere projection). The double couple (DC) portion is 92% and the seismic moment M_o is estimated as $8.5 \cdot 10^{14}$ Nm ($M_w = 3.9$). The oblique normal fault mechanism with a strike in NNW-SSE direction is in good agreement with the known SSW-NNE striking extensional seismotectonic regime in the LRE (Ahorner, 1994; Hinzen, 2003).

We used the full moment tensor solution for this event to compute synthetic seismograms for stations PLH and PLH-S using a reflectivity algorithm proposed by Wang (1999). The velocity model for the forward modeling consists of the minimum 1D crustal-velocity model derived for the LRE (Reamer and Hinzen, 2001) with modifications in the upper 195 m to include the shallow shear wave velocity structure derived from ambient vibration data (Scherbaum et al., 2003). The P-wave velocities in the sediment layer were chosen according to a power-law function determined empirically by Budny (1984) for the LRE via non-linear regression from all downhole measurements in this region. The parameters of the velocity

Table 2 - Layered velocity model used for modeling theoretical seismograms at the Pulheim site. The shear-velocity depth profile derived in Scherbaum et al. (2003) from ambient vibration data is used to model the sediment structure. Compressional wave velocities for the sediments are taken from Budny (1984), whereas the crustal model resembles the minimum 1D reference model for the LRE (Reamer and Hinzen, 2001).

H [km]	V_P [km/s]	V_S [km/s]	ρ [g/cm3]	Q_P	Q_S
0.000 - 0.010	0.701	0.270	1.70	40	20
0.010 - 0.020	1.676	0.332	2.10	40	20
0.020 - 0.040	1.784	0.396	2.10	60	30
0.040 - 0.060	1.837	0.430	2.10	60	30
0.060 - 0.080	1.873	0.454	2.10	100	50
0.080 - 0.100	1.900	0.473	2.10	100	50
0.100 - 0.120	1.922	0.488	2.10	100	50
0.120 - 0.140	1.940	0.501	2.10	100	50
0.140 - 0.160	1.956	0.513	2.10	100	50
0.160 - 0.180	1.970	0.523	2.10	100	50
0.180 - 0.195	1.981	0.531	2.10	100	50
0.195 - 1.000	5.500	3.161	2.70	200	100
1.000 - 2.000	5.750	3.305	2.70	1000	500
2.000 - 4.000	5.980	3.437	2.80	1000	500
4.000 - 10.00	6.110	3.512	2.80	1000	500
10.00 - 18.00	6.300	3.621	2.85	1000	500
18.00 - 26.00	6.360	3.655	2.90	1000	500
26.00 - 30.00	7.350	4.224	2.95	1000	500
30.00 -	8.050	4.626	3.34	1000	500

model are given in Table 2. As a source time function for the seismogram computation, we used a Brüstle-Müller model (Brüstle and Müller, 1983) with a corner frequency of 3 Hz.

In Fig. 6, we compare the synthetic 3-component seismograms in the ZRT coordinate system to the recordings at borehole station PLH and the LE3D-5s seismometer P06G. To facilitate phase and amplitude comparisons, we first simulated all seismograms (synthetic and observed) to the common instrument response of the LE3D-5s instrument. Furthermore, we applied a 4th-

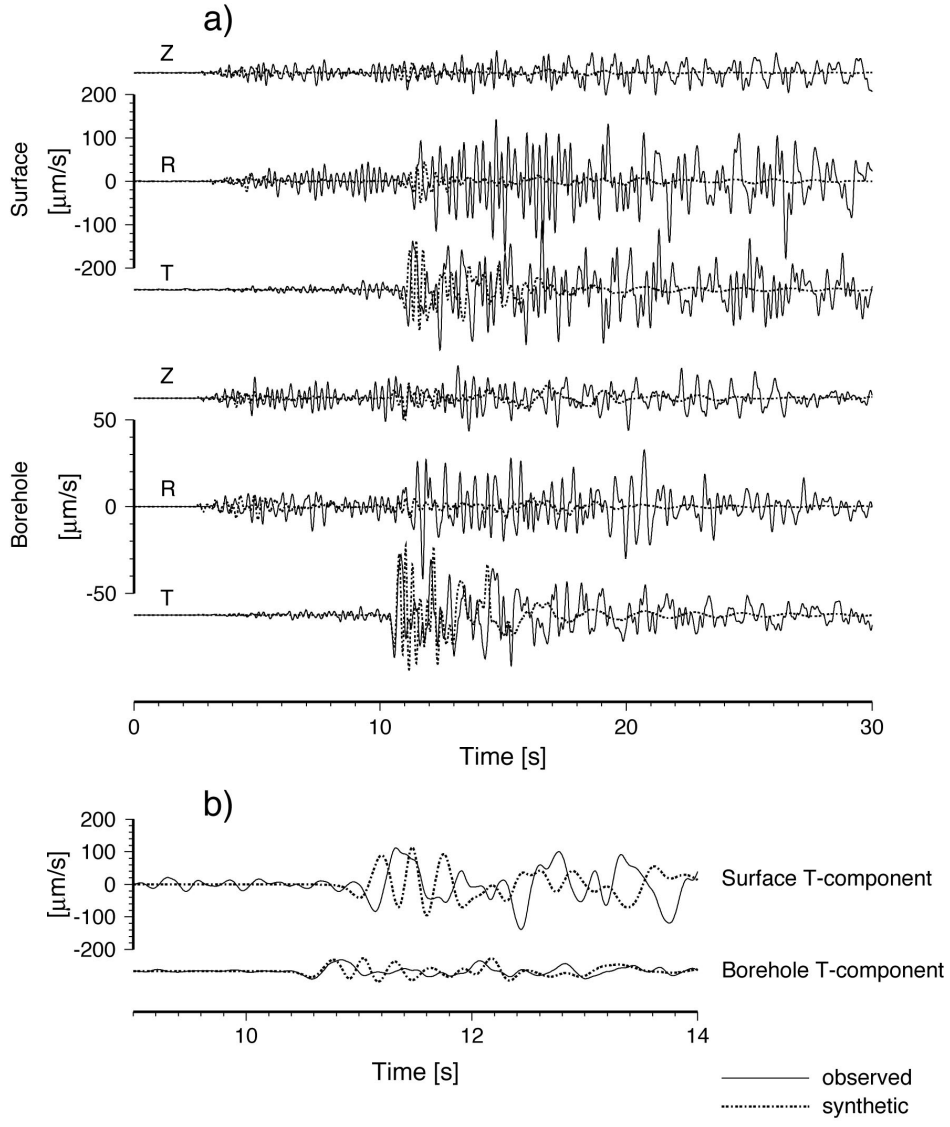

Fig. 6 - Comparison of observed seismograms (solid lines) and reflectivity synthetics (dashed lines) for borehole station PLH and surface station P06G. Seismograms have been simulated to a common seismometer response (P06G, 0.2 Hz seismometer, 70.7% critical damping) and further bandpassed between 0.2 Hz and 5 Hz. The traces have been aligned to the S-wave at the borehole station. a) Z,R,T components of surface and borehole station, superimposed on the synthetic waveforms. Amplitude scales have been selected individually for the surface and downhole station to enable detailed waveform comparison. b) SH-wave windows of T-components. The arrival of the modeled seismogram at the surface station is clearly too early with respect to the observed data.

order Butterworth bandpass filter with corner frequencies 0.2 Hz and 5 Hz to all data. As expected, due to the use of the regional crustal velocity model and possible hypocentral location errors, the absolute travel times of P- and S-waves (t_P, t_S) and $t_P - t_S$ for the synthetic seismograms do not fit the observed travel times perfectly. We therefore aligned the seismograms to the onset of the SH-wave arrival of the downhole station PLH (T-component) in order to allow a quantitative comparison of the relative S-wave time-delays caused by the overlying velocity structure only, and to further facilitate a waveform comparison for the S-wave train. We reduced the theoretical seismograms to 60% of their original amplitudes to better resemble the observed S-wave amplitudes. The overestimation of amplitudes by a factor of 1.5 is probably due to high Q values introduced for deeper crustal layers in the velocity model ($Q_P = 1000$, $Q_S = 500$), amplitude reduction of the observed direct S-wave due to scattering effects and, as the observation angle at PLH is close to a nodal plane, small misorientation of the focal mechanism and directivity effects due to rupture propagation.

At first glance, we find similar features between the predicted and observed seismograms (Fig. 6). The S-wave amplitude ratios between surface and borehole station, as well as the amplitude ratios between the individual components are in good agreement with the observed data (note that scales are different for borehole and surface stations). However, obvious discrepancies are observed regarding the complexity and length of the S-wave coda. This can be attributed to the use of a simplified homogeneous 1D-structure for modeling which neglects scattering and reverberations caused by the 3D-structure of the sedimentary basin (Ewald et al., 2003). An unexpected misfit occurs for the delay times of the SH-wave between borehole and surface station when compared between theoretical and observed seismograms. The theoretical delay time is shorter than the actual observed one, as represented by $(t_{SH}^{top} - t_{SH}^{bottom})_{obs} - (t_{SH}^{top} - t_{SH}^{bottom})_{theo} \approx 0.18\ s$.

We consider an underestimation of the sediment thickness in the ambient vibration model as the most likely explanation for the measured travel-time delay. The difficulties of estimating the sediment/bedrock interface depth when inverting the dispersion curve and HVSR have already been noted in Scherbaum et al. (2003). For the Pulheim site, for example, the insertion of a transitional sediment layer of 100 m thickness between the proposed sediment model and the halfspace slightly decreased the overall misfit in the inversion. Extending the proposed power-law model by approximately 100 m would explain the observed travel-time delays. The observed travel time residual could alternatively be explained by reducing the shear-wave velocities of the proposed model. In order to explain the observed time delay by the sediment structure ($h < 195$) alone, we determined a necessary change in the average shear-wave velocity $\overline{V_S}$ of 30% (from 460 m/s to 320 m/s). This, however, is not supported by the observed dispersion curve data. Therefore, we regard the explanation of the travel-time delay caused by an inaccurate estimate of the sediment shear-wave velocities as unlikely. Tentatively, changing the underlying crustal model between the depth of the borehole instrument (350 m) and the sediment/bedrock interface (195 m), we end up with unreasonable shear wave velocity estimates of V_S (bedrock) less than 1000 m/s. Similarly, allocating the accumulated travel time delay in equal parts to travel paths both in the sediment and the bedrock leads to unlikely shear-wave velocities.

4. Local earthquake analysis: surface /downhole spectral ratios

For a final test, we used the records of the 11 local earthquakes (Table 1 for parameters and Fig. 1 for geographical distribution) at the 3-component borehole station PLH and the accelerometer PLH-S at the surface to calculate spectral ratios for the SH-wave window. We adopted the following processing scheme: a) simulation of a common instrument response (in order to reduce the effects of a longer period noise, we used the surface accelerometer as the reference instrument); b) rotation in an R-T coordinate system by minimizing the T-energy of the P-wave arrivals in different frequency bands in order to account for deviations from great-circle paths caused by lateral heterogeneities of the velocity structure (borehole station only to provide a stable estimate); c) computation of spectra for SH time windows taken from the transverse component for nine different window lengths ranging from 3 s to 19 s (cosine taper and zero-padding to common FFT-length of 8192 samples); d) calculation of spectral ratios between top and bottom after applying a smoothing window (Konno and Ohmachi, 1998) to the individual spectra.

The resulting spectral ratios (SRs) show stable results for the frequency range from approximately 0.4 Hz to above 10 Hz. We carefully compared the stability of results with respect to the length of the processing window for each event (e.g. for the Heerlen earthquake shown in Fig. 7a). Except for some instabilities of the SR shapes for longer periods (> 1 s) for very short time windows (3 s and 5 s) that are due to insufficient spectral resolution, we obtained very similar results, regardless of the window length. Comparing the SR of individual events and choosing equal window lengths for the processing, the amplitude scatter in the observations are larger, but no significant differences of the amplification peak positions from event to event (see e.g. Fig. 7b for 9 s time window) were observed. For an empirical estimate of the site amplification function for Pulheim (spectral response of the layered structure between borehole depth and surface), we averaged the SR estimates of all events and for all window lengths (Fig. 7c). In order to check the accuracy of the shear-wave velocity model derived from ambient vibration measurements, we computed the SH-wave transfer function for vertical incidence via the Thomson-Haskell formalism (Thomson, 1950; Haskell, 1953). Allowing a 5% standard deviation for all layer parameters, we performed a Monte Carlo simulation assuming independent, normally distributed random variables around their respective means as given in Table 2. The sample size for the simulation has been set to 500. In Fig. 7d we compare the results from the Monte Carlo computation with the overall average obtained from the SR for the local earthquakes.

From Fig. 7d we recognize a clear shift of the position of fundamental and higher frequency peaks of the SR towards lower frequencies when compared to the Monte Carlo simulation results. We dismiss the explanation that such discrepancies are caused by interference between the upgoing and downgoing wavefields as described by Steidl et al. (1996) and Archuleta and Steidl (1998). The influence of the downgoing wavefield on SRs cannot be observed for deeper borehole stations (z > 200 m), as the downgoing wavefield is strongly attenuated in the very shallow part of the sediments as reported recently by Bonilla et al. (2002) for the Garner Valley downhole array. As an independent check, using the synthetic waveform data modeled for the

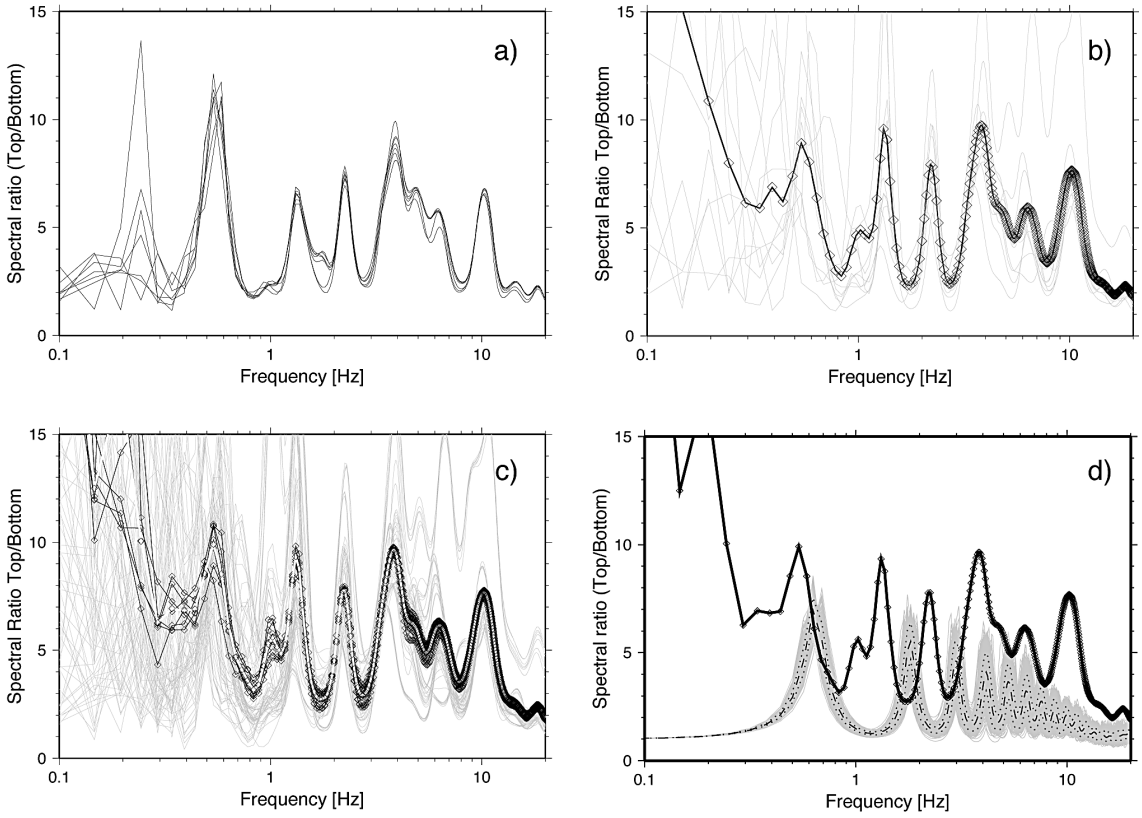

Fig. 7 - SRs for S-wave windows on T-component between surface station PLH-S and borehole station PLH: a) SR for event 0882 (Heerlen mainshock) estimated from variable window lengths; b) SR computed for a window length of 9 s for all 11 events in Table 1 (grey lines), connected diamonds show the average taken for the complete set of events; c) grey lines: all SR estimates for all processing lengths and events; black lines: average SR for each individual event, taken over all windows; white line: overall average; d) comparison of overall average SR (as in sub-figure c) to a Monte Carlo simulation (gray: individual samples, black solid: sample mean, black dashed: sample standard deviation) of the SH-transfer function computed for the shear-wave velocity model derived from ambient vibration measurements for the Pulheim site (Scherbaum et al., 2003). The standard deviation for the variation of all layer parameters in the simulation has been set to 5% of the mean value.

Heerlen mainshock, we computed SR for the synthetic data in the same way as for the earthquake records. Although we used much higher Q-values than those proposed by Budny (1984) in the velocity model, we obtained a very good match of the SR to the site amplification functions derived from the Monte Carlo simulation. No significant influence of the downgoing wavefield was observed. We also interpret the good agreement as an indication of the appropriateness of the adopted processing scheme.

We opt for a deeper sediment/bedrock interface depth than the one obtained from the inversion of ambient vibration measurements to better explain the SR derived from earthquake data. In Fig. 8a we depict the results from a Monte Carlo run for an adjusted velocity model. By extending the layer thickness of the deepest sediment layer (as given in Table 2) by 50 m from 15 m to 65 m (compare also Fig. 8b), we were able to successfully model the position of the fundamental peak at 0.50-0.55 Hz. The correspondence of resonance frequency and travel times

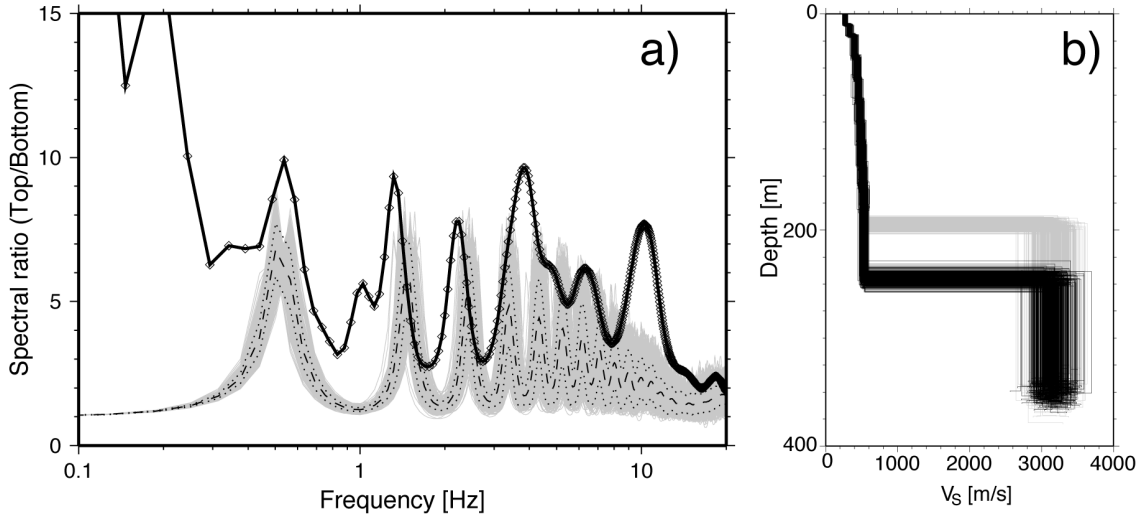

Fig. 8 - a) comparison of average SR from local earthquake data and a Monte Carlo simulation of the vertical SH-transfer function (as in Fig. 7d). The model has been adjusted to better match the observed SR. b) comparison of shear-wave model distribution used in the simulation run for Figs. 7d (grey) and 8a (black). The sediment/bedrock interface has been shifted downwards by 50 m. For details, see text.

within the sedimentary layer suggested to re-compute the synthetic waveforms for this modified model. As expected, we obtained a reduction of the shear-wave travel time residual by 0.1 s from 0.18 s to 0.08 s, whereas the amplitude ratios and waveforms did not change significantly.

However, the spectral peaks at 1.30-1.35 Hz and 2.2-2.3 Hz still deviate slightly from higher fundamentals of the simulation at 1.45-1.50 Hz and 2.40-2.50 Hz. The prominent peaks around 3.8 Hz and 10.2 Hz observed for the SR derived from earthquake data have no correspondence to the theoretical site amplification functions. We propose the existence of an internal structure in the very shallow part of the velocity model ($h < 20$ m) with significant impedance contrasts which cannot be appropriately modeled by the smooth power-law model class used for the combined inversion. With respect to the amplification factors of the resolvable spectral peaks (fundamental and first two overtones), we observe an underestimation of the amplitudes by a factor of approximately 30% from our model. However, it should again be noted, that we had already used a low-attenuating velocity model here (high Q-values).

5. Discussion and conclusions

We tested the reliability of shallow shear-wave velocity models derived from ambient vibrations in the LRE by independent tests. We performed a direct comparison of shear-wave velocity models derived from passive microtremor recordings and active downhole measurements (Budny, 1984) at one site in the LRE (Jülich). Considering the limitations of the model class used for the combined inversion scheme (Scherbaum et al., 2003), we find an excellent match with the independently derived models. This result is different from findings of Wills (1998) and Boore and Brown (1998), who reported significant differences between shear-

wave velocity profiles derived from surface-wave analysis and down- or cross-hole measurements in California. It must be noted that the surface-wave analysis results, subject of the research papers of Wills (1998) and Boore and Brown (1998), stem from active experiments and differ with respect to the target depths of investigation (upper tens of meters) in comparison to our study (< 200-300 m). As we lack detailed background information about those experiments and the processing details which led to the reported systematic overestimation of shear wave velocities from surface wave analysis methods, we can only speculate about the cause. As shown in the work of Tokimatsu et al. (1992) and Tokimatsu (1997), we postulate the existence of a mixing of fundamental and higher-mode dispersion curves, which would result in overestimation of phase velocity estimates in the dispersion data and could remain undetected by the analyst's quality control. The apparent match between down-hole measurements and shear wave velocity profiles derived from ambient vibration data in this study might therefore be a validation of the assumption that the observed ambient noise wavefield in the LRE is composed mainly of fundamental mode Rayleigh waves at least for the frequency band presented in this study.

On the other hand, testing the shear-wave velocity profile derived from ambient vibration measurements at the Pulheim site by analysis of local earthquake recordings, produced discrepancies with respect to both the SH-wave travel times for the upper 350 m as well as the peak frequencies of the site amplification function predicted from our model. Even though we cannot completely dismiss an overestimation of shear-wave velocities in our ambient vibration model, we consider the required relative average velocity reduction to explain the observed travel time delays as too high to be compatible with the observed dispersion data. We find it most likely that an incorrect estimate of the sediment/bedrock interface depth is the explanation for the mismatch between the predictions from the shallow, shear-wave velocity model and observations from local earthquake recordings. First, as has been noted in Scherbaum et al. (2003), the estimate of the sediment thickness is less well constrained than the absolute values of the velocity-depth model. Secondly, the insertion of a transitional layer into the velocity model led to a decrease of the misfit function in the inversion, although this result was not regarded as significant at that time. Moreover, the stratigraphy of the borehole at Pulheim shows the strongest impedance contrast, the interface between the tertiary sediment fill and Paleozoic bedrocks at a depth of 257 m (Rolf Pelzing, pers. comm.). According to the borehole log, the bedrock at this depth consists of weathered carbonic rock extending down to a depth of 300 m, where solid rocks of Devonian age have been drilled down to the depth of the borehole station at 350 m. This independent information supports the adjustment in sediment/bedrock interface depth in the ambient vibration model to match the observed site amplification functions obtained from the local earthquakes.

As has been proposed by Boore and Brown (1998), the best way to compare different estimates of shear-wave velocity profiles is to use the site amplification functions predicted by the models under consideration. In this study, we tested the reliability of shear-wave velocity models obtained from inversion of ambient vibration data in the LRE directly from the observed and predicted site responses at the Pulheim site. Although we obtained a mismatch of ca. 0.05 to 0.10 Hz between the observed and predicted spectral peak locations for the fundamental

frequency, we consider the average shape and the amplitudes of the predicted site amplification frequencies below 2 Hz as sufficiently close to the observed site responses to be regarded as useful. However, both the observed strong amplifications for frequencies around 3.8 Hz and 10.2 Hz, as well as the underestimation of the sediment thickness, which causes the mismatch in the spectral peak location of the fundamental frequency, leads to the conclusion that improvements to the method are necessary to fully rely on shear-wave velocity models derived from ambient vibration data.

We attribute the site amplification mismatch for the higher spectral peaks to the use of a highly simplified and smooth velocity-depth power-law function for the inversion, that fails to accurately model the apparent existence of stronger impedance contrasts in the very shallow part (< 20 m) of the site structure. Additionally, the band-limitations of the available dispersion curve data for the inversion (0.70-2.2 Hz at site Pulheim) limits the accuracy of shear-wave velocity estimates for both the shallowest and deepest parts of the model. We therefore propose to use a more flexible parametrization approach of the velocity structure during the inversion procedure (e.g. Wathelet et al., 2003) and additionally to extend the valid frequency band of the dispersion data through improvements in the measurement strategy.

Acknowledgments. We are indebted to Daniel Vollmer for the continuous maintenance of the instruments and his support and helping hands during the ambient vibration measurements. We thank P.-Y. Bard for a copy of his SH-transfer function code. All maps and figures were generated with the Generic Mapping Tools GMT (Wessel and Smith, 1991). M. Ohrnberger has been financed by EU-Grant No. EVG1-CT-2000-00026 (SESAME). Preliminary results of this study were presented at the 28th ESC General Assembly, September 1-6, 2002, held in Genoa, Italy, and the 3rd Forum of the German Committee for Disaster Reduction held in Potsdam, Germany, October 7-9, 2002. We are grateful for the comments and suggestions of D. Slejko, F. Luzón Martínez and W. Crawford which considerably helped to clarify and to improve the script.

References

Ahorner L.; 1994: *Fault-plane solutions and source parameters of the 1992 Roermond, the Netherlands, mainshock and its stronger aftershocks from regional seismic data*. Geologie en Mijnbouw, Special Issue, **73**, 199-214.

Aki K. and Richards P.G.; 1980: *Quantitative Seismology*. W.H. Freeman and Company, New York, 932 pp.

Archuleta R.J. and Steidl J.H.; 1998: *ESG studies in the United States: results from borehole arrays*. In: Irikura K., Kudo K., Okada H. and Satasini T. (eds), The Effects of Surface Geology on Seismic Motion, Balkema, Rotterdam, pp. 3-14.

Bard P.-Y.; 1998: *Microtremor measurements: a tool for site effect estimation?* In: Irikura K., Kudo K., Okada H. and Satasini T. (eds), The Effects of Surface Geology on Seismic Motion, Balkema, Rotterdam, pp. 1251-1279.

Bonilla L.F., Steidl J.H., Gariel J.-Ch. and Archuleta R.J.; 2002: *Borehole response studies at the Garner Valley downhole array, southern California.* Bull. Seism. Soc. Am., **92**, 3165-3179.

Boore D.M. and L.T. Brown; 1998: *Comparing shear-wave velocity profiles from inversion of surface-wave phase velocities with downhole measurements: systematic differences between CXW method and downhole measurements at six USC strong-motion sites*. Seismol. Res. Lett., **69**, 222-229.

Borcherdt R.D.; 1970: *Effects of local geology on ground motion near San Francisco Bay*. Bull. Seism. Soc. Am., **60**, 29-61.

Borcherdt R.D. and Gibbs J.F.; 1976: *Effects of local geological conditions in the San Francisco Bay region on ground motions and the intensities of the 1906 earthquake*. Bull. Seism. Soc. Am., **66**, 467-500.

Brüstle W. and Müller G.; 1983: *Moment and duration of shallow earthquakes from Love-wave modeling for regional distances*. Phys. Earth and Planet. Interiors, **32**, 312-324.

BSSC, Building Seismic Safety Council; 2001: *The 2000 NEHRP recommended provisions for new buildings and other structures, 2000 Edition, Part 1: Provisions*. (FEMA 368), Washington, D.C.

Budny M.; 1984: *Seismische Bestimmung der bodendynamischen Kennwerte von oberflächennahen Schichten in Erdbebengebieten der Niederrheinischen Bucht und ihre ingenieurseismologische Anwendung*. Ph.D. Thesis Special publications No. 57, Geologisches Institut der Universität zu Köln, 209 pp. (in German).

Campbell K.W.; 1976: *A note on the distribution of earthquake damage in Long Beach, 1933*. Bull. Seism. Soc. Am., **86**, 1001-1006.

Capon J.; 1969: *High-resolution frequency-wavenumber spectrum analysis*. Proc. IEEE, **57**, 1408-1418.

ESG; 1998: *Proceedings of the Second International Symposium on the Effects of surface geology on seismic motion*. Yokohama, Balkema, 3 Volumes.

Ewald M., Igel H., Hinzen K.-G. and Scherbaum F.; 2003: *3D finite-difference modeling of earthquakes in the Cologne basin, Germany*. Geophys. Res. Abstr., **5**, EAE03-A-08964.

Fäh D., Kind F. and Giardini D.; 2001: *A theoretical investigation of average H/V ratios*. Geophys. J. Int., **145**, 535-549.

Gao S., Liu H., Davis P.M. and Knopoff L.; 1996: *Localized amplification of seismic waves and correlation with damage due to the Northridge earthquake: evidence for focusing in Santa Monica*. Bull. Seism. Soc. Am., **86**, S209-S230.

Hartzell S., Leeds A., Frankel A. and Michael J.; 1996: *Site response for urban Los Angeles using aftershocks of the Northridge earthquake*. Bull. Seism. Soc. Am., **86**, S168–S192.

Haskell N.A.; 1953: *The dispersion of surface waves on multilayered media*. Bull. Seism. Soc. Am., **43**, 17-34.

Hinzen K.-G.; 2003: *Stress field in the northern Rhine area, central Europe, from earthquake fault plane solutions*. Tectonophysics, **377**, 325-356.

Hinzen K.-G., Scherbaum F. and Weber B.; 2003: *On the resolution of H/V measurements to determine sediment thickness, a case study across a normal fault in the Lower Rhine Embayment, Germany.* J. Earth. Eng., submitted.

Horike M.; 1985: *Inversion of phase velocity of long-period microtremors to the S-wave velocity structure down to the basement in urbanized areas*. J. Phys. Earth., **33**, 59-96.

Ibs von Seht M. and Wohlenberg R.; 1999: *Microtremor measurements used to map thickness of soft soil sediments*. Bull. Seism. Soc. Am., **89**, 250-259.

Ishida H., Nozawa T. and Niwa M.; 1998: *Estimation of deep surface structure based on phase velocities and spectral ratios of long-period microtremors*. In: Second International Symposium on the Effects of Surface Geology on Seismic Motion, Yokohama, Balkema, **2**, pp. 697-704.

Konno K. and Ohmachi T.; 1998: *Ground-motion characteristics estimated from spectral ratio between horizontal and vertical components of microtremor*. Bull. Seism. Soc. Am., **88**, 228-241.

Krüger F. and Dahm T.; 2002: *The 1992 Roermond earthquake, a regional event study*. In: Ten years of German Regional Seismic Network (GRSN), Senate Commission for Geosciences, Report 25, Wiley Vch Verlags GmbH, pp. 199-206.

Kværna T. and Ringdahl F.; 1986: *Stability of various f-k estimation techniques*. In: Semiannual technical summary, 1 October 1985 - 31 March 1986, NORSAR Scientific Report, 1-86/87, Kjeller, Norway, pp. 29-40.

Parolai S., Bormann P. and Milkereit C.; 2002: *New relationships between vs, thickness of sediments, and resonance frequency calculated by the H/V ratio of seismic noise for Cologne area (Germany)*. Bull. Seism. Soc. Am., **92**, 2521-2527.

Pelzing R.; 1990: *The seismic network of the Geological Survey of North Rhine-Westfalia and the seismic activity of the Lower Rhine area from 1980 to 1988*. In: Camelbeeck T., Flick J. and Ducarme B. (eds), Seismic networks and digital data transmission and exchange, Cah. Centre Europ. Géodyn. Séismol., **1**, Centre Europ. Géodyn. Séismol., Luxembourg, pp. 75-84.

Reamer Sh.-K. and Hinzen K.-G.; 2001: *Evaluation of the phase data catalog for the station Bensberg for the years 1970-2000*. In: DGG - 61st Annual Meeting, Frankfurt am Main, 19.03.-23.03.2001.

Satoh T., Kawase H. and Matsushima Sh.; 2001a: *Estimation of S-wave velocity structures in and around the Sendai Basin, Japan, using array records of microtremors*. Bull. Seism. Soc. Am., **91**, 206-218.

Satoh T., Kawase H., Iwata T., Higashi S., Sato T., Irikura K. and Huang H.-Ch.; 2001b: *S-wave velocity structure of the Taichung Basin, Taiwan, estimated from array and single-station records of microtremors*. Bull. Seism. Soc. Am., **91**, 1267-1282.

Scherbaum F., Hinzen K.-G. and Ohrnberger M.; 2003: *Determination of shallow shear wave velocity profiles in the Cologne, Germany area using ambient vibrations*. Geophys. J. Int., **152**, 597-612.

Schlittenhardt J.; 1999: *Regional velocity models for Germany: a contribution to the systematic travel-time calibration of the International Monitoring System*. In: Proceedings of the 21st Seismic Research Symposium: Technologies for Monitoring the Comprehensive Nuclear Test Ban Treaty, Las Vegas, Nevada, vol. 1, pp. 263-273.

Steidl J.H., Tumarkin A.G. and Archuleta R.J.; 1996: *What is a reference site?* Bull. Seism. Soc. Am., **86**, 1733-1748.

Thomson W.T.; 1950: *Transmission of elastic waves through a stratified solid medium*. J. Appl. Phys., **21**, 89-93.

Tokimatsu K., Shinzawa K. and Kuwayama S.; 1992: *Use of short-period microtremors for vs profiling*. J. Geotech. Eng., **118**, 1544-1558.

Tokimatsu K.; 1997: *Geotechnical site characterization using surface waves*. In: Ishihara K. (ed), Earthquake Geotechnical Engineering, Balkema, Rotterdam, pp. 1333-1368.

Wang R.; 1999: *A simple orthonormalization method for stable and efficient computation of Green's functions*. Bull. Seism. Soc. Am., **89**, 733-741.

Wathelet M., Jongmans D. and Ohrnberger M.; 2003: *Surface wave inversion using a direct search algorithm and its application to ambient vibration measurements*. Near Surface Geophysics, submitted.

Welch P.D.; 1967: *The use of Fast Fourier Transform for the estimation of power spectra: a method based on time averaging over short, modified periodograms*. IEEE Trans. Audio Elect.-Acoust., AU-15, 70-73.

Wessel P. and Smith W.H.F.; 1991: *Free software helps map and display data*. Eos, Trans. Am. Geophys. U., **72**, 444-446.

Wills C.J.; 1998: *Differences in shear-wave velocity due to measurement methods: a cautionary note*. Seism. Res. Lett., **69**, 217-221.

Yamanaka H.; 1998: *Geophysical explorations of sedimentary structures and their characterization*. In: Irikura K., Kudo K., Okada H., and Satasini T. (eds), The Effects of Surface Geology on Seismic Motion, Balkema, Rotterdam, pp. 15-33.